

Role of trap-induced scales in non-equilibrium dynamics of strongly interacting trapped bosons

Anirban Dutta,¹ Rajdeep Sensarma,² and K. Sengupta¹

¹*Theoretical Physics Department, Indian Association for the Cultivation of Science, Jadavpur, Kolkata-700032, India.*

²*Department of Theoretical Physics, Tata Institute of Fundamental Research, Mumbai-400005, India.*

(Dated: January 14, 2022)

We use a time-dependent hopping expansion technique to study the non-equilibrium dynamics of strongly interacting bosons in an optical lattice in the presence of a harmonic trap characterized by a force constant K . We show that after a sudden quench of the hopping amplitude J across the superfluid (SF)-Mott insulator (MI) transition, the SF order parameter $|\Delta_r(t)|$ and the local density fluctuation $\delta n_r(t)$ exhibit sudden decoherence beyond a trap-induced time scale $T_0 \sim K^{-1/2}$. We also show that after a slow linear ramp down of J , $|\Delta_r|$ and the boson defect density P_r display a novel non-monotonic spatial profile. Both these phenomena can be explained as consequences of trap-induced time and length scales affecting the dynamics and can be tested by concrete experiments.

PACS numbers: 75.10.Jm, 05.70.Jk, 64.60.Ht

The study of non-equilibrium dynamics of closed quantum many-body systems has gained tremendous momentum in recent years [1], mainly due to experiments on ultracold atoms in optical lattices [2–6]. Isolation from external baths and long timescales for dynamics in these ultra low temperature systems make it easy to follow the system in real time without ultrafast probes. Ultracold atoms can be used to emulate several strongly correlated quantum Hamiltonians like the Ising and the Bose-Hubbard (BH) models, which are known to undergo quantum phase transitions [7–9] as a function of easily tuneable parameters. Experiments on these systems provide a unique opportunity to study non-equilibrium dynamics of strongly interacting quantum many-body systems in the vicinity of quantum critical points.

The experimental setup of ultracold atoms inevitably has a harmonic trapping potential, which provides the largest lengthscale in the problem. In equilibrium, the trap: (a) smears out phase transitions into crossovers, as the long wavelength low energy “critical” fluctuations are cut-off at the trap lengthscale and (b) realizes multiple phases like a Mott insulator (MI) and a superfluid (SF) coexisting in different regions of the trap, leading to interesting phase boundaries between them. The dynamics of these strongly interacting systems in the presence of confining potentials is an interesting topic, which has implications over a wide range of physical phenomenon from dynamics of hot dense QCD matter to nuclear reactions to dynamics of early universe and so on. While the equilibrium phase diagram of ultracold atoms in presence of confining potentials is well studied, the interplay of strong interactions and confinement in the dynamics of these systems is open to new descriptions.

The BH model, emulated by the ultracold atom systems, consists of bosons hopping on a lattice with a hopping amplitude J and interacting with a local repulsion U . It supports a superfluid-insulator (SI) quantum phase transition as a function of the parameter J/U , with

the quantum critical point occurring in the strong coupling regime $U \gg J$. In this Letter, we study the non-equilibrium dynamics of this system in the presence of a harmonic trap characterized by a force constant K , when we change the hopping parameter J from an initial high value (in the equilibrium superfluid phase) to a low value (in the equilibrium Mott insulator phase) across the quantum phase transition.

We first look at the evolution of the system after an instantaneous quench of the hopping parameter. Initially the local superfluid order parameter $|\Delta_r|$ and the local density fluctuations δn_r follow the well known collapse and revival dynamics of the homogeneous system up to a trap induced time scale $T_0 \sim K^{-1/2}$. Beyond this timescale, the oscillations decohere suddenly and the system settles into a steady state. We also look at the evolution of the system through a linear ramp-down of the hopping parameter $J(t)$ with a rate τ^{-1} . We find that at the end of slow ramps ($\tau U \gg 1$), both $|\Delta_r|$ and the local defect density P_r display novel non-monotonic spatial profile as a function of r , which characterizes the highly non-equilibrium state produced at the end of the ramp. We provide a semi-analytic explanation for both the K dependence of T_0 and the non-monotonic spatial profile of $|\Delta_r|$ and P_r after the ramp in terms of trap-induced length and time scales which affect the dynamics of these systems in presence of confining potential, and suggest concrete experiments to test our theory.

We would like to note that, while several numerical and analytical methods are used to study the equilibrium properties of the SI transition in BH model for $d > 1$ [10–13], none of these can describe its non-equilibrium dynamics beyond the mean-field level. Recently, some progress has been made in this direction in Ref. [12], but treatment of dynamics of non-uniform systems are beyond that method. To the best of our knowledge, methods to address non-equilibrium dynamics of inhomogeneous BH model beyond mean-field theory do not exist

for $d > 1$ [15, 16]. Here, we develop a hopping expansion technique for strongly coupled bosons in an optical lattice in the presence of a spatially varying potential which treats the equilibrium and non-equilibrium properties of the system on an equal footing.

The BH model in the presence of a trap is given by

$$H = -J \sum_{\langle \mathbf{r}\mathbf{r}' \rangle} (b_{\mathbf{r}}^\dagger b_{\mathbf{r}'} + h.c.) + \sum_{\mathbf{r}} \frac{U}{2} \hat{n}_{\mathbf{r}}(\hat{n}_{\mathbf{r}} - 1) - \mu_{\mathbf{r}} \hat{n}_{\mathbf{r}}, \quad (1)$$

where $b_{\mathbf{r}}$ annihilates a boson at lattice site \mathbf{r} and $\hat{n}_{\mathbf{r}} = b_{\mathbf{r}}^\dagger b_{\mathbf{r}}$. Here, $\mu_{\mathbf{r}} = \mu_0 - K|\mathbf{r}|^2/2$ is the effective chemical potential at site \mathbf{r} , K is the force constant of the harmonic trap potential, and the central value μ_0 controls the total density. For concreteness, we will consider nearest neighbor hopping of bosons on a square lattice.

The BH hamiltonian can be divided into a local part H_0 , consisting of the Hubbard repulsion and the effective chemical potential term, and the kinetic hopping term T . In the strong coupling regime, a perturbation expansion in the hopping terms is obtained in the following way: Consider neighboring sites \mathbf{r} and \mathbf{r}' with occupation numbers $n_{\mathbf{r}}$ and $n_{\mathbf{r}'} = n_{\mathbf{r}} - \alpha + 1$, where α is an integer. When a boson hops from \mathbf{r}' to \mathbf{r} , the energy change $\Delta E_{\mathbf{r}\mathbf{r}'}^\alpha = \alpha U - \mu_{\mathbf{r}} + \mu_{\mathbf{r}'}$. It is thus useful to consider the hopping terms corresponding to the same α together and write: $T = \sum_{\langle \mathbf{r}\mathbf{r}' \rangle} T_{\mathbf{r}\mathbf{r}'} = \sum_{\langle \mathbf{r}\mathbf{r}' \rangle \alpha} (T_{\mathbf{r}\mathbf{r}'}^\alpha + T_{\mathbf{r}'\mathbf{r}}^{-\alpha})$, where

$$T_{\mathbf{r}\mathbf{r}'}^\alpha = -J \sum_{n_{\mathbf{r}}} \sqrt{(n_{\mathbf{r}} + 1)(n_{\mathbf{r}} + 1 - \alpha)} |n_{\mathbf{r}} + 1, n_{\mathbf{r}} - \alpha\rangle \times \langle n_{\mathbf{r}}, n_{\mathbf{r}} - \alpha + 1|. \quad (2)$$

For a given pair of \mathbf{r} and \mathbf{r}' , the low energy process corresponds to $\bar{\alpha}_{\mathbf{r}\mathbf{r}'}$, for which $\Delta E_{\mathbf{r}\mathbf{r}'}^{\bar{\alpha}_{\mathbf{r}\mathbf{r}'}} < \gamma J$, where γ is a number $\mathcal{O}(1)$ [17]. The rest of the terms are taken as high energy processes to be eliminated by a canonical transformation. Note that there can be pairs of sites where all hopping processes are high energy terms, and hence there are no terms $\mathcal{O}(J)$ in the effective Hamiltonian between these sites. A binary variable $\eta_{\mathbf{r}\mathbf{r}'}$, which is 1(0) if the corresponding bond has (does not have) a low energy hopping term, is used to keep track of this.

Having identified the high-energy hopping processes for which $\alpha_{\mathbf{r}\mathbf{r}'} \neq \bar{\alpha}_{\mathbf{r}\mathbf{r}'}$, one can now design a canonical transformation operator S which eliminate these processes perturbatively to obtain an effective Hamiltonian $H_{\text{eff}} = \exp(iS)H\exp(-iS)$. To linear order in J , this requires $[H_0, iS] = \sum_{\langle \mathbf{r}\mathbf{r}' \rangle \alpha \neq \bar{\alpha}_{\mathbf{r}\mathbf{r}'}} (T_{\mathbf{r}\mathbf{r}'}^\alpha + T_{\mathbf{r}'\mathbf{r}}^{-\alpha})$ and yields

$$iS = \sum_{\langle \mathbf{r}\mathbf{r}' \rangle} \sum_{\alpha \neq \bar{\alpha}_{\mathbf{r}\mathbf{r}'}} (T_{\mathbf{r}\mathbf{r}'}^\alpha - T_{\mathbf{r}'\mathbf{r}}^{-\alpha}) / \Delta E_{\mathbf{r}\mathbf{r}'}^\alpha. \quad (3)$$

where we have used the fact that $\bar{\alpha}_{\mathbf{r}\mathbf{r}'} = -\bar{\alpha}_{\mathbf{r}'\mathbf{r}}$.

Using the above S , the effective low-energy Hamiltonian H_{eff} for the trapped bosons, to $\mathcal{O}(z^2 J^2/U^2)$, is

$$H_{\text{eff}} = H_0 + \sum_{\langle \mathbf{r}\mathbf{r}' \rangle} [T_{\mathbf{r}\mathbf{r}'}^{\bar{\alpha}_{\mathbf{r}\mathbf{r}'}} + T_{\mathbf{r}'\mathbf{r}}^{-\bar{\alpha}_{\mathbf{r}\mathbf{r}'}}] \eta_{\mathbf{r}\mathbf{r}'} \quad (4)$$

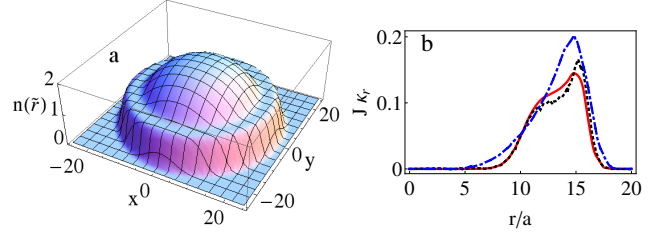


FIG. 1: (Color online) (a): Density profile of the bosons in a 2D harmonic trap with $\mu_0 = 1.4U$ and $Ka^2 = 0.006U$ (b): Plot of $J\kappa_{\mathbf{r}}$ (red solid curve) as a function of the distance from the trap center, r_0 , for $\mu_0/U = 0.37$ and $Ka^2 = 0.002U$ showing comparison with QMC data (black dotted curve) and mean-field theory (blue dash-dotted curve). $J = 0.04U$ and $N = 51 \times 51$ for both plots.

$$+ \sum_{\langle \mathbf{r}\mathbf{r}' \rangle \langle \mathbf{r}_1\mathbf{r}_2 \rangle} \eta_{\mathbf{r}\mathbf{r}'} \sum_{\alpha \neq \bar{\alpha}_{\mathbf{r}_1\mathbf{r}_2}} \frac{[T_{\mathbf{r}_1\mathbf{r}_2}^\alpha - T_{\mathbf{r}_2\mathbf{r}_1}^{-\alpha}, T_{\mathbf{r}\mathbf{r}'}^{\bar{\alpha}_{\mathbf{r}\mathbf{r}'}} + T_{\mathbf{r}'\mathbf{r}}^{-\bar{\alpha}_{\mathbf{r}'\mathbf{r}}}]}{\Delta E_{\mathbf{r}_1\mathbf{r}_2}^\alpha} \\ + \sum_{\langle \mathbf{r}\mathbf{r}' \rangle \langle \mathbf{r}_1\mathbf{r}_2 \rangle} \sum_{\alpha \neq \bar{\alpha}_{\mathbf{r}_1\mathbf{r}_2} \beta \neq \bar{\beta}_{\mathbf{r}\mathbf{r}'}} \frac{[T_{\mathbf{r}_1\mathbf{r}_2}^\alpha - T_{\mathbf{r}_2\mathbf{r}_1}^{-\alpha}, T_{\mathbf{r}\mathbf{r}'}^{\bar{\beta}} + T_{\mathbf{r}'\mathbf{r}}^{-\bar{\beta}}]}{2\Delta E_{\mathbf{r}_1\mathbf{r}_2}^\alpha}.$$

We first use this formalism to look at the equilibrium ground state of the trapped system. We use a variational wavefunction ansatz, $|\psi\rangle = \exp(-iS)|\psi'\rangle$, where $|\psi'\rangle = \prod_{\mathbf{r}} \sum_{n_{\mathbf{r}}} f_{n_{\mathbf{r}}}^{\mathbf{r}} |n_{\mathbf{r}}\rangle$ is a Gutzwiller wavefunction, $n_{\mathbf{r}}$ is the local boson occupation number basis, and the variational Gutzwiller coefficients $f_{n_{\mathbf{r}}}^{\mathbf{r}}$ are determined by minimizing the ground state energy $E_G = \langle \psi | H | \psi \rangle = \langle \psi' | H_{\text{eff}} | \psi' \rangle + \mathcal{O}(z^3 J^3/U^2)$ [18]. We note that in our approach, $|\psi\rangle$, unlike $|\psi'\rangle$, retains spatial correlations due to the $\exp(iS)$ factor. The ground state expectation value of any operator \hat{O} to $\mathcal{O}(J^2/U^2)$ is then given by

$$\langle \psi | \hat{O} | \psi \rangle = \langle \psi' | e^{iS} \hat{O} e^{-iS} | \psi' \rangle + \mathcal{O}(z^3 J^3/U^3). \quad (5)$$

The ground state density profile for a system of 51×51 lattice sites is shown in Fig. 1(a). It shows the wedding cake structure with the $n_{\mathbf{r}} = \langle \hat{n}_{\mathbf{r}} \rangle = 2$ central Mott lobe surrounded by a SF ring and then the $n_{\mathbf{r}} = 1$ Mott lobe, as we go towards the edge of the trap. To make quantitative comparison between this method, Quantum Monte Carlo (QMC) [19] and mean-field theory [10], we plot in Fig. 1(b), the local compressibility $\kappa_{\mathbf{r}} = \langle \psi | \hat{n}_{\mathbf{r}}^2 | \psi \rangle - n_{\mathbf{r}}^2$ of the system as a function of $r_0 = |\mathbf{r}|$. In this case, we use $\mu_0 = 0.37U$ so that we only have a $n = 1$ central Mott lobe. The comparison shows that our method provides a more accurate match with QMC data than the mean-field theory in the MI and MI-SF transition regions.

We now turn to the description of the non-equilibrium dynamics of this system as the hopping is changed according to an arbitrary protocol $J(t)$. The Schrodinger equation is given by $i\hbar \partial_t |\psi(t)\rangle = H[J(t)] |\psi(t)\rangle$. Following Ref. [12], we work with a time-dependent canonical transformation $S[J(t)]$, i.e. $|\psi(t)\rangle = e^{iS[J(t)]} |\psi'(t)\rangle$.

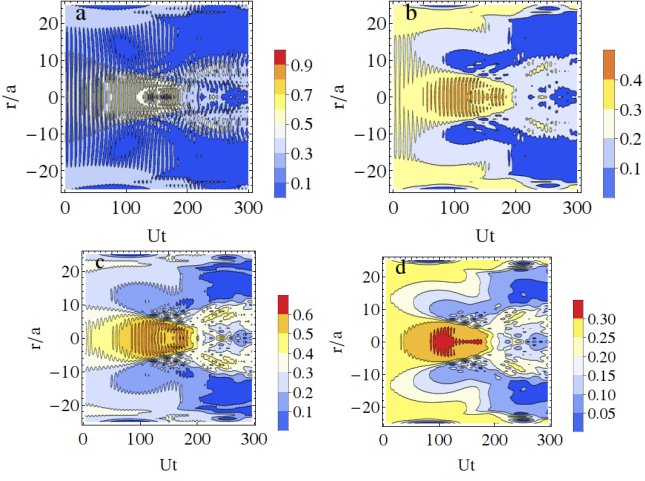


FIG. 2: (Color online) Time evolution after a sudden quench of J from $J_i = 0.1U$ to $J_f = 0.02U$: (a) $|\Delta_r(t)|$ and (b) $\delta n_r(t)$ as a function of r and t . (c) and (d): Same as (a) and (b) respectively, but integrated over a timescale $\delta t = 2\pi/U$ to show the slow dynamics clearly.

The basic idea is to keep the fast oscillating (high energy) terms within the canonical transformation, so that $|\psi'(t)\rangle$ can encode the slow motion generated by the time-dependent effective Hamiltonian $H_{\text{eff}}[J(t)]$ (given by Eq. 5 with $J \rightarrow J(t)$). The Schrodinger equation then reduces to

$$(i\hbar\partial_t + \hbar\partial S/\partial t)|\psi'(t)\rangle = H_{\text{eff}}[J(t)]|\psi'(t)\rangle. \quad (6)$$

We then use a time dependent Gutzwiller ansatz $|\psi'(t)\rangle = \prod_{\mathbf{r}} \sum_{n_{\mathbf{r}}} f_{n_{\mathbf{r}}}^{\mathbf{r}}(t) |n_{\mathbf{r}}\rangle$ and obtain the differential equations for $f_{n_{\mathbf{r}}}^{\mathbf{r}}(t)$ [18]. These are solved numerically to obtain the time dependent state $|\psi(t)\rangle$ [20].

First, we concentrate on the sudden quench of J from $J = J_i$, where the bosons in the trap center are in the SF phase, to $J = J_f$, where the ground state at the trap center is a MI with $\bar{n} = 1$. In Fig. 2(a), we plot the spatio-temporal profile of $|\Delta_r(t)|$, where $\Delta_r(t) = \langle \psi(t) | b_r | \psi(t) \rangle$ is the local superfluid order parameter, and r is the distance from the trap center along $(1, 0)$. It shows prominent oscillations with a frequency $\sim U^{-1}$, corresponding to the coherent collapse and revival of the superfluid state in the center. Around $T_0 \sim 1/K^{1/2}$, these oscillations suddenly decohere very fast and soon the system settles into a steady state pattern. This decoherence is not the exponential decay due to hopping, but is precipitated by a catastrophic event which immediately causes loss of coherence. A similar pattern is seen in the local density fluctuations $\delta n_r(t)$, plotted in Fig. 2(b). In Figs. 2(c) and (d), we plot the spatio-temporal profile of $|\Delta_r(t)|$ and $\delta n_r(t)$, after smearing over a time grid $\delta t \sim U^{-1}$ to clearly visualize long time-scale dynamics of the system, showing how it settles into the steady state.

To obtain a qualitative understanding of this phe-

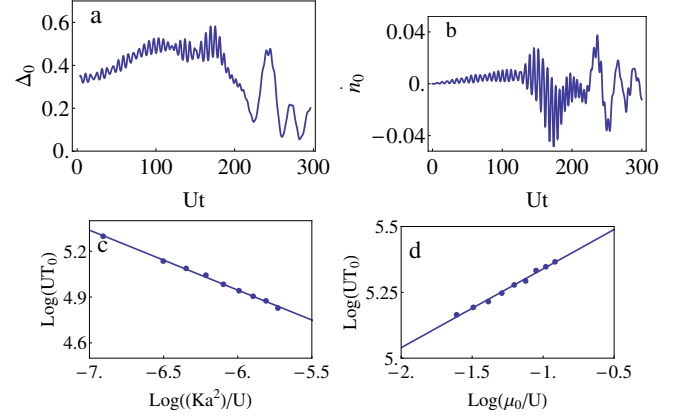


FIG. 3: (Color online) Time evolution of (a) $|\Delta_0(t)|$ and (b) $\dot{n} \equiv \dot{n}_{r=0}(t)$ at the trap center after a sudden quench of J from $J_i = 0.1U$ to $J_f = 0.02U$. (c) and (d) Plot of $\ln(T_0U)$ as a function of $\ln(Ka^2/U)$ and $\ln(\mu_0/U)$ respectively. The straight lines in (c) and (d) show linear fit to the data points.

nomenon, we note that the trap leads to actual mass (particle) transport with a typical velocity $v_b \simeq J_f/\hbar$ (where the optical lattice spacing is set to unity) affecting the dynamics of the system [15, 16]. When a boson hops outwards from a site r along $(1, 0)$ direction, it encounters the boundary between the SF and the $n = 0$ MI phase at $\mu_r = 0$ or at $r = \text{Int}[\sqrt{2\mu_0/K}]$. Since the latter phase is analogous to the boson vacuum, the bosons get reflected back from this boundary. When the reflected wave reaches a given point inside the boundary, it interferes with the coherent oscillation and causes it to decohere. To see this process clearly, we plot in Fig. 3(a) and (b), the SF order parameter $|\Delta|$ and the time derivative of the boson density, \dot{n} , at the trap center as a function of time. We clearly see that the sudden decoherence of $|\Delta(t)|$ coincides with an increase in \dot{n} . The reflection of the bosons leads to inhomogeneous boson flux at a given site leading, via continuity equation, to finite \dot{n} and hence to decoherence of the short time oscillation pattern of $|\Delta_{r=0}(t)|$. For the central trap site, we expect this to happen around $T_0 \simeq 2r_x^{\text{max}}/J_f = 2\text{Int}[\sqrt{2\mu_0/K}]/J_f \simeq 200U^{-1}$ [21]. Our reasoning above predicts $T_0 \sim 1/\sqrt{K}$ and $T_0 \sim \sqrt{\mu_0}$; this is corroborated in Figs. 3(c) and 3(d). These plots indicate $T_0 \sim K^{-0.53}$ and $T_0 \sim \mu^{0.41}$ which is roughly consistent with the behavior $1/\sqrt{K}$ and $\sqrt{\mu_0}$ obtained from our qualitative argument.

Finally, we study the effect of a linear ramp-down of the hopping $J(t) = J_i + (J_f - J_i)t/\tau$ in this system. We choose $J_i(J_f) = 0.1(0.02)U$ so that the bosons start from the SF ground state and pass through the equilibrium MI-SF transition for $r < 14$. For $14 \leq r \leq 20$ ($r > 20$), the equilibrium state of the bosons are SF ($n = 0$ MI) state throughout the dynamics. We look at the system at the end of the ramp ($t = \tau$) and study the local order parameter $|\Delta_r(\tau)|$ and the local defect density $P_r(\tau) =$

$1 - |\langle \psi_r(\tau) | \psi_{rG} \rangle|^2$, where $|\psi_{rG}\rangle$ is the ground state with $J = J_f$ and $|\psi_r(\tau)\rangle$ is the non-equilibrium state right after the ramp. As shown in Fig. 4(a) and (b), $|\Delta_r(\tau)|$ and $P_r(\tau)$ display non-monotonic spatial profiles for large τ (close to adiabatic limit); they have a maximum at $r = 0$ followed by an initial reduction and later enhancement as r increases. We note that such spatial profiles have no analog for trapped bosons in equilibrium.

To understand these novel profiles, we first consider the behavior of $|\Delta_r(\tau)|$ and $P_r(\tau)$ near the trap center where the effect of the trap potential is negligible. Here, for a slow quench, one can use an adiabatic-impulse argument to estimate the deviation of the final wavefunction from the initial one [22]. The evolution of the wavefunction gets the system in the adiabatic regime (no defect production) when the instantaneous energy gap $\epsilon(t)$ satisfies $d\epsilon/dt \leq \epsilon(t)^2$. Near the trap center, we can use LDA to define a local gap, $\epsilon_r(t) = \text{Min}[E_r^p(t), E_r^h(t)]$, where $E_r^p(t) = U - \mu_r - 2zJ(t)$ and $E_r^h(t) = \mu_r - zJ(t)$ are energies of particle/hole production. The time at which the system enters the adiabatic regime, t_1 , can be obtained by solving $d\epsilon(t)/dt|_{t=t_1} = \epsilon^2(t_1)$ and yields

$$t_1(r) = \tau[J_i - J_{cr}(r)](J_i - J_f)^{-1} + \sqrt{\tau/(J_i - J_f)} \quad (7)$$

where $J_{cr}(r) = \text{Min}[(U - \mu_r)/2z, \mu_r/z]$ is the equilibrium critical value of J at the local effective potential $\mu(r)$. For our choice of parameters, $J_{cr}(r)$ decreases with r ; consequently, t_1 is an increasing function of r . Thus the trap center $r = 0$ spends minimum time in the so called impulse region, where the local wavefunction can adjust to the changes in J . Thus the deviation of the wavefunction from the initial superfluid state is minimum here. Hence $|\Delta_r(\tau)|$ has a maxima at $r = 0$ and gradually decreases with r with the profile of $|\Delta_r(\tau)|$ having the same shape as J_{cr} . The defect density profile near the trap center can also be understood from the same argument if we remember that the defect density measures the deviation of the state from the ground state with the final value of J , and not from the initial state. Since the freeze-out occurs later as we go outward, the states at larger r are closer to the final ground state and has less defect density.

However, the effect of larger time spent in the impulse region is offset by the slower evolution due to the presence of the trap as we move outward from the trap center. To understand this, consider the Gutzwiller mean-field theory of trapped boson with $J = J(t)$. Using a minimal model of three boson states near SI transition, $n = 0, 1, 2$ per site [18, 23], the wavefunction $\psi_{\text{mf}} = \prod_r \sum_{n_r=0}^2 c_{n_r}^{\mathbf{r}}(t) |n\rangle$. In this limit, $\Delta_{\mathbf{r}}(t) = \Delta_{1\mathbf{r}}(t)e^{-i\mu_{\mathbf{r}}t/\hbar} + \Delta_{2\mathbf{r}}(t)e^{-i(U-\mu_{\mathbf{r}})t/\hbar}$ [18], where, within a rotating wave approximation,

$$\dot{\Delta}_{1[2]\mathbf{r}}(t) = -iJ(t) \sum_{\langle \mathbf{r}' \rangle} |c_1^{\mathbf{r}'}|^2 A_{\mathbf{r}\mathbf{r}'}(t) [B_{\mathbf{r}\mathbf{r}'}(t)] e^{i\delta\mu_{\mathbf{r}}t/\hbar} \quad (8)$$

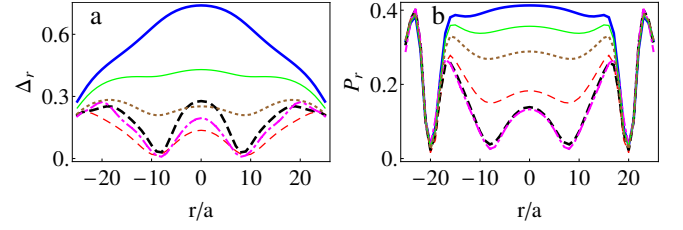


FIG. 4: (Color online) Spatial profile of (a) the order parameter amplitude $|\Delta_r|$ and (b) defect density P_r after a linear ramp of J from $J_i = 0.1U$ to $J_f = 0.02U$. The different curves correspond to $U\tau = 1$ (blue solid line), 2 (green solid line), 3 (brown dotted line), 5 (orange dashed line), 10 (pink dash-dotted line), and 15 (black dashed line).

Here ℓ denotes the link between \mathbf{r} and \mathbf{r}' , and the coefficients $A_{\mathbf{r}\mathbf{r}'} = c_0^{\mathbf{r}*} c_1^{\mathbf{r}'}$ and $B_{\mathbf{r}\mathbf{r}'} = \sqrt{2} c_1^{\mathbf{r}*} c_2^{\mathbf{r}'}$. It can be seen from Eq. 8 that for $t > t_0$, where t_0 is defined by $J(t_0) = \delta\mu_{\ell}$, the oscillatory terms would wash out the dynamics of $|\Delta|$. Thus one expects the evolution of Δ_r to be small at sites for which t_0 is small compared to the ramp time τ . It is easy to see numerically that $J(t_0) = J_f$ for $r \simeq 9$. It is approximately around this point that the slow nature of the evolution overcompensates for larger time spent in the impulse region and one finds an upturn of the order parameter. Further, we expect the dynamics to become progressively slower as we move further outwards. Consequently, $|\Delta_r(\tau)|$ increases with r for $8 \leq r \leq 19$. A similar behavior is seen for the defect density P_r . For $r > 19$, the small initial $|\Delta_r(0)|$, owing to the proximity of the system to the $n = 0$ MI phase, outweighs the slow evolution during ramp dynamics and thus both $|\Delta_r(\tau)|$ and $P_r(\tau)$ again starts to decrease.

Experimental verification of our theory can be most easily done by using standard parity of occupation measurements [4, 24] which would capture the non-monotonic dependence of P_r after the ramp. This would require inference of P_r from the experimentally measured parity of boson occupation. We note that this can be easily done using techniques of Ref. [4] since only states with $n_r \leq 2$ bosons have appreciable weights in the regime $U \gg J$.

In conclusion, we have presented a novel hopping expansion techniques which allows us to address the non-equilibrium dynamics of trapped bosons in the strong coupling regime beyond mean-field theory. We have identified a trap-induced length scale $r_{\text{max}} \sim 1/\sqrt{K}$, which acts as a reflection boundary for the dynamics of the bosons after the quench leading to a sudden decoherence of the collapse revival oscillations at $T_0 \sim K^{-1/2}$. In evolution under a slow linear ramp of J , we have found a novel non-monotonic spatial profile of the defect density and order parameter amplitude which is qualitatively different from its counterpart in equilibrium and can be measured easily by available experiments.

AD acknowledges helpful discussions with Juan Car-

rasquilla at early stages of this project.

SUPPLEMENTARY MATERIAL: SKETCH OF THE VARIATIONAL ENERGY CALCULATION

In this section, we provide a sketch of the calculation of the variational energy $E_G = \langle \psi' | H_{\text{eff}} | \psi' \rangle$ used in the main text. We first write the effective Hamiltonian as

$$\begin{aligned} H_{\text{eff}} &= H_{\text{eff}}^0 + H_{\text{eff}}^1 + H_{\text{eff}}^2, \\ H_{\text{eff}}^0 &= \sum_{\mathbf{r}} \left[-\mu_{\mathbf{r}} \hat{n}_{\mathbf{r}} + \frac{U}{2} \hat{n}_{\mathbf{r}} (\hat{n}_{\mathbf{r}} - 1) \right] \\ H_{\text{eff}}^1 &= \sum_{\ell, i=1,2} T_{\ell i}^{\bar{\alpha}_{\ell i}} \eta_{\bar{\alpha}_{\ell i}} \\ H_{\text{eff}}^2 &= \sum_{\ell \ell'} \sum_{\alpha \neq \bar{\alpha}_{\ell i}} \sum_{i,j=1,2} \eta_{\bar{\alpha}_{\ell i}} [T_{\ell' j}^{\alpha}, T_{\ell i}^{\bar{\alpha}_{\ell i}}] / \Delta E_{\ell' j}^{\alpha} \quad (9) \\ &\quad + \sum_{\ell \ell'} \sum_{\alpha \neq \bar{\alpha}_{\ell i}, \alpha' \neq \bar{\alpha}_{\ell' j}} \sum_{i,j=1,2} [T_{\ell i}^{\alpha}, T_{\ell' j}^{\alpha'}] / (2\Delta E_{\ell i}^{\alpha}), \end{aligned}$$

where we have introduced the link variable ℓ between two neighboring sites \mathbf{r} and \mathbf{r}' , ℓ' denote either the same link as or the nearest neighbor link of ℓ , $\Delta E_{\ell}^{\alpha} = \alpha U - \mu_{\mathbf{r}} + \mu_{\mathbf{r}'}$, and $\eta_{\bar{\alpha}_{\ell i}} = 0(1)$ if $\bar{\alpha}_{\ell i}$ exists (does not exist) for a given link. The definition of all other operators used in Eq. 9 is given in the main text. In terms of these link variables, one can distinguish between the outward and inward hopping processes on link as $T_{\ell 1}$ and $T_{\ell 2}$ respectively. The hopping term can be then written as $T = \sum_{\ell} T_{\ell} = \sum_{\ell \alpha} T_{\ell 1}^{\alpha} + T_{\ell 2}^{\alpha}$, where

$$\begin{aligned} T_{\ell 1}^{\alpha} &= -J \sum_{n_{\mathbf{r}}} \sqrt{n_{\mathbf{r}}(n_{\mathbf{r}} + \alpha)} |n_{\mathbf{r}} - 1, n_{\mathbf{r}} + \alpha\rangle \\ &\quad \times \langle n_{\mathbf{r}}, n_{\mathbf{r}} + \alpha - 1|, \\ T_{\ell 2}^{\alpha} &= -J \sum_{n_{\mathbf{r}}} \sqrt{(n_{\mathbf{r}} + 1)(n_{\mathbf{r}} + 1 - \alpha)} |n_{\mathbf{r}} + 1, n_{\mathbf{r}} - \alpha\rangle \\ &\quad \times \langle n_{\mathbf{r}}, n_{\mathbf{r}} - \alpha + 1|. \end{aligned} \quad (10)$$

$$E_G^1 = -J \sum_{n_{\mathbf{r}} \ell} \left[\eta_{\bar{\alpha}_{\ell 1}} \sqrt{n_{\mathbf{r}}(n_{\mathbf{r}} + \bar{\alpha}_{\ell 1} - 1)} f_{n_{\mathbf{r}}-1}^{*\mathbf{r}} f_{n_{\mathbf{r}}}^{\mathbf{r}} f_{n_{\mathbf{r}}+\bar{\alpha}_{\ell 1}}^{*\mathbf{r}'} f_{n_{\mathbf{r}}+\bar{\alpha}_{\ell 1}-1}^{\mathbf{r}'} + \eta_{-\bar{\alpha}_{\ell 1}} \sqrt{n_{\mathbf{r}}(n_{\mathbf{r}} + \bar{\alpha}_{\ell 1} + 1)} f_{n_{\mathbf{r}}+1}^{*\mathbf{r}} f_{n_{\mathbf{r}}}^{\mathbf{r}} f_{n_{\mathbf{r}}+\bar{\alpha}_{\ell 1}}^{*\mathbf{r}'} f_{n_{\mathbf{r}}+\bar{\alpha}_{\ell 1}+1}^{\mathbf{r}'} \right], \quad (16)$$

where we have used $\bar{\alpha}_{\ell 2} = -\bar{\alpha}_{\ell 1}$, \mathbf{r}' is the neighboring site of \mathbf{r} , and ℓ denotes the link between these two sites.

Next, we discuss computation of terms $O(J^2/U^2)$.

We note that Eq. 10 is analogous to Eq. (2) of the main text. Also, it is worth noting that in this representation, one can write

$$iS = \sum_{\ell} \sum_{i=1,2} \sum_{\alpha \neq \bar{\alpha}_{\ell i}} T_{\ell i}^{\alpha} / \Delta E_{\ell i}^{\alpha}. \quad (11)$$

which has been used to derive Eq. 9. Using Eq. 9, one can express the variational ground state energy as

$$E_G = \sum_{\alpha=0,1,2} E_G^{\alpha}, \quad E_G^{\alpha} = \langle \psi' | H_{\text{eff}}^{\alpha} | \psi' \rangle, \quad (12)$$

where $|\psi'\rangle$ is the Gutzwiller wavefunction given by

$$|\psi'\rangle = \prod_{\mathbf{r}} \sum_{n_{\mathbf{r}}} f_{n_{\mathbf{r}}}^{\mathbf{r}} |n_{\mathbf{r}}\rangle \quad (13)$$

We begin with computation E_G^0 . Since this term involves only density operators on a single site, it is straightforward to see that

$$E_G^0 = \sum_{n_{\mathbf{r}}} \sum_{\mathbf{r}} |f_{n_{\mathbf{r}}}^{\mathbf{r}}|^2 \left[-\mu_{\mathbf{r}} n_{\mathbf{r}} + \frac{U}{2} n_{\mathbf{r}} (n_{\mathbf{r}} - 1) \right] \quad (14)$$

To compute E_G^1 , which involves terms involving a single link and hence two adjacent sites, we first note that using Eq. 2 of the main text, one can write

$$\begin{aligned} T_{\ell 1}^{\alpha} |n_1, n_2\rangle &= -J \sum_{n_{\mathbf{r}}} \delta_{n_{\mathbf{r}}, n_1} \delta_{n_{\mathbf{r}}+\alpha-1, n_2} \sqrt{n_{\mathbf{r}}(n_{\mathbf{r}} + \alpha)} \\ &\quad \times |n_{\mathbf{r}} - 1, n_{\mathbf{r}} + \alpha\rangle \\ T_{\ell 2}^{\alpha} |n_1, n_2\rangle &= -J \sum_{n_{\mathbf{r}}} \delta_{n_{\mathbf{r}}, n_1} \delta_{n_{\mathbf{r}}-\alpha+1, n_2} \\ &\quad \times \sqrt{(n_{\mathbf{r}} + 1)(n_{\mathbf{r}} - \alpha)} |n_{\mathbf{r}} + 1, n_{\mathbf{r}} - \alpha\rangle \end{aligned} \quad (15)$$

where \mathbf{r} denotes a site of the link ℓ . Using Eq. 15, one can obtain $E_G^1 = \langle \psi' | \sum_{\ell, i=1,2} T_{\ell i}^{\bar{\alpha}_{\ell i}} \eta_{\bar{\alpha}_{\ell i}} | \psi' \rangle$ to be

$$T_{\ell 1}^{\alpha} T_{\ell 1}^{\beta} |n_1, n_2\rangle = J^2 \delta_{\beta, \alpha-2} \delta_{n_2, n_1+\alpha-3} \sqrt{n_1(n_1-1)(n_2+1)(n_2+2)} |n_1-2, n_2+2\rangle$$

$$\begin{aligned}
T_{\ell_1}^\alpha T_{\ell_2}^\beta |n_1, n_2\rangle &= J^2 \delta_{\beta, -\alpha} \delta_{n_2, n_1 + \alpha + 1} n_2 (n_1 + 1) |n_1, n_2\rangle \\
T_{\ell_2}^\alpha T_{\ell_1}^\beta |n_1, n_2\rangle &= J^2 \delta_{\beta, -\alpha} \delta_{n_2, n_1 - \alpha - 1} n_1 (n_2 + 1) |n_1, n_2\rangle \\
T_{\ell_2}^\alpha T_{\ell_2}^\beta |n_1, n_2\rangle &= J^2 \delta_{\beta, \alpha - 2} \delta_{n_2, n_1 - \alpha + 3} \sqrt{(n_1 + 1)(n_1 + 2)(n_2 - 1)n_2} |n_1 + 2, n_2 - 2\rangle.
\end{aligned} \tag{17}$$

For example, using these one can compute one of the representative terms in the expression of E_G^2 as $E_{G(1)}^2 =$

$\langle \psi' | \sum_{\ell \neq \pm \bar{\alpha}_{\ell_1}} T_{\ell_1}^\alpha (T_{\ell_1}^{\bar{\alpha}_{\ell_1}} + T_{\ell_2}^{-\bar{\alpha}_{\ell_1}}) / \Delta E_{\ell_1}^\alpha | \psi' \rangle$. A few lines of straightforward algebra yields

$$E_{G(1)}^2 = \sum_{\ell, n_{\mathbf{r}}} \sum_{\alpha \neq \pm \bar{\alpha}_{\ell_1}} \frac{J^2 \eta_{\bar{\alpha}_{\ell_1}}}{\Delta E_{\ell_1}^{\bar{\alpha}_{\ell_1} + 2}} f_{n_{\mathbf{r}} - 2}^{*\mathbf{r}} f_{n_{\mathbf{r}}}^{\mathbf{r}} f_{n_{\mathbf{r}} + \bar{\alpha}_{\ell_1}}^{*\mathbf{r}'} f_{n_{\mathbf{r}} + \bar{\alpha}_{\ell_1} - 1}^{\mathbf{r}'} \sqrt{n_{\mathbf{r}}(n_{\mathbf{r}} + 1)(n_{\mathbf{r}} + \bar{\alpha}_{\ell_1})(n_{\mathbf{r}} + \bar{\alpha}_{\ell_1} + 1)} \tag{18}$$

All others terms with $\ell = \ell'$ which contribute to E_G^2 can be computed in an analogous fashion.

Next, we consider the terms in E_G^2 which originates from terms in H_2 which has ℓ and ℓ' as neighboring links. For these terms, one involves three lattice sites which have coordinates \mathbf{r} , \mathbf{r}' , and \mathbf{r}'' . We use the convention

that the link between sites with coordinates \mathbf{r} and \mathbf{r}' is ℓ and that \mathbf{r}' is the middle site connecting the link ℓ and ℓ' . With this convention, there are two classes of hopping terms. In the first of these classes, $T_{\ell'}$ acts on the state $|\psi'\rangle$ before T_ℓ leading to the following relations:

$$\begin{aligned}
T_{\ell_1}^\alpha T_{\ell'_1}^\beta |n_1, n_2, n_3\rangle &= J^2 \delta_{n_2, n_1 + \alpha} \delta_{n_3, n_2 + \beta - 1} n_2 \sqrt{n_1(n_1 + 1)} |n_1 - 1, n_2, n_3 + 1\rangle \\
T_{\ell_1}^\alpha T_{\ell'_2}^\beta |n_1, n_2, n_3\rangle &= J^2 \delta_{n_2, n_1 + \alpha - 2} \delta_{n_3, n_2 - \beta + 1} \sqrt{(n_2 + 1)(n_2 + 2)n_1 n_3} |n_1 - 1, n_2 + 2, n_3 - 1\rangle \\
T_{\ell_2}^\alpha T_{\ell'_1}^\beta |n_1, n_2, n_3\rangle &= J^2 \delta_{n_2, n_1 - \alpha + 2} \delta_{n_3, n_2 - \beta + 1} \sqrt{n_2(n_2 - 1)(n_1 + 1)(n_3 + 1)} |n_1 + 1, n_2 - 2, n_3 + 1\rangle \\
T_{\ell_2}^\alpha T_{\ell'_2}^\beta |n_1, n_2, n_3\rangle &= J^2 \delta_{n_2, n_1 - \alpha} \delta_{n_3, n_2 - \beta + 1} n_2 \sqrt{n_3(n_1 + 1)} |n_1 + 1, n_2, n_3 - 1\rangle.
\end{aligned} \tag{19}$$

In the second class of terms, T_ℓ acts on $|\psi'\rangle$ before $T_{\ell'}$ and this leads to

$$\begin{aligned}
T_{\ell'_1}^\alpha T_{\ell_1}^\beta |n_1, n_2, n_3\rangle &= T_{\ell_1}^{\beta - 1} T_{\ell'_1}^{\alpha + 1} |n_1, n_2, n_3\rangle, \\
T_{\ell'_1}^\alpha T_{\ell'_2}^\beta |n_1, n_2, n_3\rangle &= T_{\ell'_2}^{\beta + 1} T_{\ell'_1}^{\alpha - 1} |n_1, n_2, n_3\rangle, \\
T_{\ell'_2}^\alpha T_{\ell_1}^\beta |n_1, n_2, n_3\rangle &= T_{\ell_1}^{\beta + 1} T_{\ell'_2}^{\alpha - 1} |n_1, n_2, n_3\rangle, \\
T_{\ell'_2}^\alpha T_{\ell'_2}^\beta |n_1, n_2, n_3\rangle &= T_{\ell'_2}^{\beta - 1} T_{\ell'_2}^{\alpha + 1} |n_1, n_2, n_3\rangle.
\end{aligned}$$

Using these identities one can evaluate the contribution of all terms in H_2 with $\ell \neq \ell'$ to E_G^2 . A representative example of such a term is $E_{G(2)}^2 = \langle \psi' | \sum_{(\ell \ell')} \sum_{\alpha \neq \pm \bar{\alpha}_{\ell_1}} T_{\ell_1}^\alpha (T_{\ell'_1}^{\bar{\alpha}_{\ell'_1}} + T_{\ell'_2}^{-\bar{\alpha}_{\ell'_1}}) / \Delta E_{\ell_1}^\alpha | \psi' \rangle$. A straightforward calculation using Eq. 19 yields

$$\begin{aligned}
E_{G(2)}^2 &= \sum_{(\ell \ell'), n_{\mathbf{r}}} \sum_{\alpha \neq \bar{\alpha}_{\ell'_1}} \frac{J^2}{\Delta E_{\ell_1}^\alpha} \left[\eta_{\bar{\alpha}_{\ell'_1}} f_{n_{\mathbf{r}} - 1}^{*\mathbf{r}} f_{n_{\mathbf{r}}}^{\mathbf{r}} |f_{n_{\mathbf{r}} + \alpha}^{\mathbf{r}'}|^2 f_{n_{\mathbf{r}} + \alpha + \bar{\alpha}_{\ell'_1}}^{*\mathbf{r}''} f_{n_{\mathbf{r}} + \alpha + \bar{\alpha}_{\ell'_1} - 1}^{\mathbf{r}''} \sqrt{n_{\mathbf{r}}(n_{\mathbf{r}} + \alpha + \bar{\alpha}_{\ell'_1})} \right. \\
&\quad \left. + \eta_{-\bar{\alpha}_{\ell'_1}} f_{n_{\mathbf{r}} - 1}^{*\mathbf{r}} f_{n_{\mathbf{r}}}^{\mathbf{r}} f_{n_{\mathbf{r}} + \alpha}^{*\mathbf{r}'} f_{n_{\mathbf{r}} + \alpha - 1}^{\mathbf{r}'} f_{n_{\mathbf{r}} + \alpha + \bar{\alpha}_{\ell'_1} - 2}^{*\mathbf{r}''} f_{n_{\mathbf{r}} + \alpha + \bar{\alpha}_{\ell'_1} - 1}^{\mathbf{r}''} \sqrt{n_{\mathbf{r}}(n_{\mathbf{r}} + \alpha)(n_{\mathbf{r}} + \alpha - 1)(n_{\mathbf{r}} + \alpha + \bar{\alpha}_{\ell'_1} - 1)} \right]
\end{aligned} \tag{21}$$

All other terms with $\ell \neq \ell'$ can be obtained in a similar fashion using Eqs. 19 and 20. Together, these terms

leads to the expression of E_G^2 used in the main text. The ground state wavefunction, used for obtaining Fig. 1 in

the main text, is obtained by numerical minimization of E_G .

To obtain the numerical solution of the time-dependent Schrödinger equation $(i\hbar\partial_t + \partial_t S[J(t)])|\psi'\rangle = H_{\text{eff}}[J(t)]|\psi'\rangle$ used in the main text, we first write $|\psi'\rangle = \prod_{\mathbf{r}} \sum_{n_{\mathbf{r}}} f_{n_{\mathbf{r}}}^{\mathbf{r}}(t)|n_{\mathbf{r}}\rangle$. Using standard procedure [12], it is then straightforward to obtain the equations for time evolution of $f_{n_{\mathbf{r}}}^{\mathbf{r}}(t)$ which is given by

$$\begin{aligned} i\hbar\partial_t f_{n_{\mathbf{r}}}^{\mathbf{r}}(t) &= \delta E_G[\{f_{n_{\mathbf{r}}}^{\mathbf{r}}\}; J(t)]/\delta f_{n_{\mathbf{r}}}^{*\mathbf{r}}(t) + i\hbar\dot{J}(t) \\ &\times \sum_{\alpha\langle\mathbf{r}'\rangle} \left[\sqrt{n_{\mathbf{r}}} f_{n_{\mathbf{r}}-1}^{\mathbf{r}} \phi_{n_{\mathbf{r}}-\alpha}^{\mathbf{r}'} + \sqrt{n_{\mathbf{r}}+1} f_{n_{\mathbf{r}}+1}^{\mathbf{r}} \phi_{n_{\mathbf{r}}+\alpha}^{*\mathbf{r}'} \right] \\ &\times \sum_{i=1,2} (1 - \delta_{\alpha\bar{\alpha}_{\ell i}})/\Delta E_{\ell i}^{\alpha}. \end{aligned} \quad (22)$$

From the expression of E_G obtained earlier, one can obtain, after some straightforward, but tedious algebra the terms $\delta E_G/\delta f_{n_{\mathbf{r}}}^{*\mathbf{r}}$. Eq. 22 is then numerically solved to obtain $f_{n_{\mathbf{r}}}^{\mathbf{r}}(t)$. This leads to $|\psi'(t)\rangle$, and consequently to $|\Delta_{\mathbf{r}}(t)\rangle$ and $\delta n_{\mathbf{r}}(t)$ used in the main text.

SUPPLEMENTARY MATERIALS: MEAN-FIELD THEORY

In this section, we present the mean-field calculation leading to Eq. 8 of the main text. To do this, let us consider the mean-field Bose-Hubbard Hamiltonian given by

$$\begin{aligned} H_{\text{mf}} &= H_0 + \sum_{\mathbf{r}} (\Delta_{\mathbf{r}}(t) b_{\mathbf{r}}^{\dagger} + \text{h.c.}) \\ \Delta_{\mathbf{r}} &= -J(t) \sum_{\langle\mathbf{r}'\rangle} \langle b_{\mathbf{r}'} \rangle \end{aligned} \quad (23)$$

where $\langle\mathbf{r}'\rangle$ denotes nearest neighbor sites \mathbf{r}' to \mathbf{r} , the time dependence of $J(t)$ is kept arbitrary for now, and the expectation is taken using the time-dependent variational Gutzwiller wavefunction $|\psi\rangle = \prod_{\mathbf{r}} \sum_{n_{\mathbf{r}}} c_{n_{\mathbf{r}}}^{\mathbf{r}}(t)|n_{\mathbf{r}}\rangle$. The corresponding mean-field equations for $c_{n_{\mathbf{r}}}^{\mathbf{r}}(t)$ is given by

$$\begin{aligned} (i\partial_t - \epsilon_{n_{\mathbf{r}}}^{\mathbf{r}}) c_{n_{\mathbf{r}}}^{\mathbf{r}} &= -J(t) \sum_{\langle\mathbf{r}'\rangle n_{\mathbf{r}'}} \left[\sqrt{n_{\mathbf{r}}(n_{\mathbf{r}'}+1)} c_{n_{\mathbf{r}}-1}^{*\mathbf{r}'} c_{n_{\mathbf{r}'}+1}^{\mathbf{r}'} \right. \\ &\left. \times c_{n_{\mathbf{r}}-1}^{\mathbf{r}} + \sqrt{n_{\mathbf{r}'}(n_{\mathbf{r}}+1)} c_{n_{\mathbf{r}'}-1}^{*\mathbf{r}'} c_{n_{\mathbf{r}}+1}^{\mathbf{r}} \right], \end{aligned} \quad (24)$$

where $\epsilon_{n_{\mathbf{r}}}^{\mathbf{r}} = -\mu_{\mathbf{r}} n_{\mathbf{r}} + U n_{\mathbf{r}}(n_{\mathbf{r}} - 1)/2$ is the local on-site energy.

To proceed further, we note that for $zJ(t)/U \ll 1$ (where z is the coordination number of the lattice) and for $0 < \mu_{\mathbf{r}}/U < 1$ (which holds for all $|\mathbf{r}| \leq 20$ in the present case), one has $c_{n_{\mathbf{r}} > 2}^{\mathbf{r}} = 0$ and $|c_1^{\mathbf{r}}| \gg |c_0^{\mathbf{r}}|, |c_2^{\mathbf{r}}|$. One can then approximate the mean-field equations for $c_{n_{\mathbf{r}} \leq 2}^{\mathbf{r}}$ to be

$$i\partial_t c_0^{\mathbf{r}} = -J(t) \sum_{\langle\mathbf{r}'\rangle} c_1^{\mathbf{r}} (c_1^{*\mathbf{r}'} c_0^{\mathbf{r}'} + \sqrt{2} c_2^{*\mathbf{r}'} c_1^{\mathbf{r}'})$$

$$\begin{aligned} (i\partial_t + \mu_{\mathbf{r}}) c_1^{\mathbf{r}} &= -J(t) \sum_{\langle\mathbf{r}'\rangle} \left[c_0^{\mathbf{r}} (\sqrt{2} c_1^{*\mathbf{r}'} c_2^{\mathbf{r}'} + c_0^{*\mathbf{r}'} c_1^{\mathbf{r}'}) \right. \\ &\left. c_2^{\mathbf{r}} (\sqrt{2} c_1^{*\mathbf{r}'} c_0^{\mathbf{r}'} + 2 c_2^{*\mathbf{r}'} c_1^{\mathbf{r}'}) \right], \end{aligned} \quad (25)$$

$$(i\partial_t - U + \mu_{\mathbf{r}}) c_2^{\mathbf{r}} = -J(t) \sum_{\langle\mathbf{r}'\rangle} c_1^{\mathbf{r}} (2 c_2^{*\mathbf{r}'} c_1^{\mathbf{r}'} + \sqrt{2} c_1^{*\mathbf{r}'} c_0^{\mathbf{r}'}),$$

We now define the slow variables $\tilde{c}_{n_{\mathbf{r}}}^{\mathbf{r}} = c_{n_{\mathbf{r}}}^{\mathbf{r}} \exp[-i(\epsilon_{n_{\mathbf{r}}}^{\mathbf{r}} + \mu_{\mathbf{r}})t]$ and obtain their equation of motion as

$$\begin{aligned} i\partial_t \tilde{c}_0^{\mathbf{r}} &= -J(t) \sum_{\langle\mathbf{r}'\rangle} \tilde{c}_1^{\mathbf{r}} e^{-i\delta\mu_{\mathbf{r}\mathbf{r}'}t} \left(\tilde{c}_1^{*\mathbf{r}'} \tilde{c}_0^{\mathbf{r}'} + \sqrt{2} \tilde{c}_2^{*\mathbf{r}'} \tilde{c}_1^{\mathbf{r}'} e^{iUt} \right) \\ i\partial_t \tilde{c}_1^{\mathbf{r}} &= -J(t) \sum_{\langle\mathbf{r}'\rangle} \left[\tilde{c}_0^{\mathbf{r}} e^{i\delta\mu_{\mathbf{r}\mathbf{r}'}t} \left(\sqrt{2} \tilde{c}_1^{*\mathbf{r}'} \tilde{c}_2^{\mathbf{r}'} e^{-iUt} + \tilde{c}_0^{*\mathbf{r}'} \tilde{c}_1^{\mathbf{r}'} \right) \right. \\ &\left. + \tilde{c}_2^{\mathbf{r}} e^{-i\delta\mu_{\mathbf{r}\mathbf{r}'}t} \left(\sqrt{2} \tilde{c}_1^{*\mathbf{r}'} \tilde{c}_0^{\mathbf{r}'} e^{-iUt} + 2 \tilde{c}_2^{*\mathbf{r}'} \tilde{c}_1^{\mathbf{r}'} \right) \right], \end{aligned} \quad (26)$$

$$i\partial_t \tilde{c}_2^{\mathbf{r}} = -J(t) \sum_{\langle\mathbf{r}'\rangle} \tilde{c}_1^{\mathbf{r}} e^{i\delta\mu_{\mathbf{r}\mathbf{r}'}t} (2 \tilde{c}_2^{*\mathbf{r}'} \tilde{c}_1^{\mathbf{r}'} + \sqrt{2} \tilde{c}_1^{*\mathbf{r}'} \tilde{c}_0^{\mathbf{r}'} e^{iUt}),$$

where $\delta\mu_{\mathbf{r}\mathbf{r}'} \equiv \delta\mu_{\ell} = \mu_{\mathbf{r}'} - \mu_{\mathbf{r}}$.

Next, we compute the expectation value of the superfluid order parameter: $\Delta_{\mathbf{r}} = \langle \psi | b_{\mathbf{r}} | \psi \rangle$. Using the expression for $|\psi\rangle$, one obtains

$$\begin{aligned} \Delta_{\mathbf{r}} &= \tilde{c}_0^{*\mathbf{r}} \tilde{c}_1^{\mathbf{r}} e^{-i\mu_{\mathbf{r}}t} + \sqrt{2} \tilde{c}_1^{*\mathbf{r}} \tilde{c}_2^{\mathbf{r}} e^{-i(U-\mu_{\mathbf{r}})t} \\ &= \Delta_{1\mathbf{r}} e^{-i\mu_{\mathbf{r}}t} + \Delta_{2\mathbf{r}} e^{-i(U-\mu_{\mathbf{r}})t} \end{aligned} \quad (27)$$

Using the expressions of $\Delta_{1(2)\mathbf{r}}$ in Eq. 27, one can now obtain their equations of motion from those of $\tilde{c}_n^{\mathbf{r}}$ ($n = 0, 1, 2$) obtained in Eq. 27. A few lines of straightforward algebra shows that in the limit when $|\tilde{c}_1^{\mathbf{r}}|^2 \gg |\tilde{c}_0^{\mathbf{r}}|^2, |\tilde{c}_2^{\mathbf{r}}|^2$, one has

$$\begin{aligned} i\partial_t \Delta_{1\mathbf{r}} &= J(t) \sum_{\langle\mathbf{r}'\rangle} |\tilde{c}_1^{\mathbf{r}}|^2 (A_{\mathbf{r}\mathbf{r}'} + e^{-iUt} B_{\mathbf{r}\mathbf{r}'}) e^{-i\delta\mu_{\mathbf{r}\mathbf{r}'}t} \\ i\partial_t \Delta_{2\mathbf{r}} &= -\sqrt{2} J(t) \sum_{\langle\mathbf{r}'\rangle} |\tilde{c}_1^{\mathbf{r}}|^2 (B_{\mathbf{r}\mathbf{r}'} + e^{iUt} A_{\mathbf{r}\mathbf{r}'}) e^{-i\delta\mu_{\mathbf{r}\mathbf{r}'}t} \end{aligned} \quad (28)$$

where $A_{\mathbf{r}\mathbf{r}'} = \tilde{c}_0^{*\mathbf{r}'} \tilde{c}_1^{\mathbf{r}}$ and $B_{\mathbf{r}\mathbf{r}'} = \sqrt{2} \tilde{c}_1^{*\mathbf{r}'} \tilde{c}_2^{\mathbf{r}}$. Using the rotating wave approximation, one can drop the terms with the factor $e^{iUt/\hbar}$ in right side of Eq. 28. This yields Eq. 8 in the main text where we have reexpressed $A_{\mathbf{r}\mathbf{r}'}$ and $B_{\mathbf{r}\mathbf{r}'}$ in terms of $c_n^{\mathbf{r}}$.

-
- [1] A. Polkovnikov, K. Sengupta, A. Silva, and M. Vengalattore, Rev. Mod. Phys. **83**, 863 (2011).
 - [2] I. Bloch, J. Dalibard, and W. Zwerger, Rev. Mod. Phys. **80**, 885 (2008).
 - [3] T. Kinoshita, T. Wenger and D. S. Weiss, Nature(London) **440**, 900 (2006).
 - [4] W. S. Bakr, A. Peng, M. E. Tai, R. Ma, J. Simon, J. I. Gillen, S. Foelling, L. Pollet, and M. Greiner, Science **329**, 547 (2010).
 - [5] N. Strohmaier, Niels Strohmaier, D. Greif, R. Jordens, L. Tarruell, H. Moritz, T. Esslinger, R. Sensarma, D.

- Pekker, E. Altman, and E. Demler, Phys. Rev. Lett. **104**, 080401 (2010).
- [6] L. E. Sadler, J. M. Higbie, S. R. Leslie, M. Vengalattore, and D. M. Stamper-Kurn, Nature **443**, 312 (2006).
- [7] M. Greiner, O. Mandel, T. Esslinger, T. W. Hansch, and I. Bloch, Nature (London) **415**, 39 (2002); C. Orzel, A. K. Tuchman, M. L. Fenselau, M. Yasuda, and M. A. Kasevich, Science **291**, 2386 (2001).
- [8] See for example, S. Sachdev, *Quantum Phase Transitions* (Cambridge University Press, Cambridge, England, 1999).
- [9] S. Sachdev, K. Sengupta, and S.M. Girvin, Phys. Rev. B **66**, 075128 (2002).
- [10] M. P. A. Fisher, P. B. Weichman, G. Grinstein, and D. S. Fisher, Phys. Rev. B **40**, 546 (1989); K. Sheshadri, H. R. Krishnamurthy, R. Pandit, and T. V. Ramakrishnan, Europhys. Lett. **22**, 257 (1993).
- [11] J. K. Freericks and H. Monien, Europhys. Lett. **26**, 545 (1994); K. Sengupta and N. Dupuis, Phys. Rev. A **71**, 033629 (2005); A. Rancon and N. Dupuis, Phys. Rev. B **83**, 172501 (2011); J. K. Freericks, H. R. Krishnamurthy, Y. Kato, N. Kawashima, and N. Trivedi, Phys. Rev. A **79**, 053631 (2009).
- [12] C. Trefzger and K. Sengupta, Phys. Rev. Lett. **106**, 095702 (2011); A. Dutta, C. Trefzger, and K. Sengupta, Phys. Rev. B **86**, 085140 (2012).
- [13] W. Krauth and N. Trivedi, Europhys. Lett. **14**, 627 (1991); B. Capogrosso-Sansone, N. V. Prokofev, and B. V. Svistunov, Phys. Rev. B **75**, 134302 (2007).
- [14] G. G. Batrouni, V. Rousseau, R. T. Scalettar, M. Rigol, A. Muramatsu, P. J. H. Denteneer, and M. Troyer, Phys. Rev. Lett. **89**, 117203 (2002).
- [15] J-S. Bernier, D. Poletti, P. Barmettler, G. Roux, and C. Kollath, Phys. Rev. A **85**, 033641 (2012)
- [16] S. S. Natu, K. R. A. Hazzard, and E. J. Mueller, Phys. Rev. Lett. **106**, 125301 (2010).
- [17] We use a value of $\gamma = 2$; we have checked that our results are insensitive to the exact choice of γ .
- [18] See supplementary materials for a detailed derivation.
- [19] O. Gygi, H. G. Katzgraber, M. Troyer, S. Wessel, and G. Batrouni, Phys. Rev. A **73**, 063606 (2006).
- [20] This procedure is justified as long as $zJ(t)/U \ll 1$ for all t and thus can be used to study the dynamics of the bosons in the SF region near the critical point.
- [21] After the quench, the bosons have a small residual energy $Q \sim |J_i - J_f|$. This shifts the reflection boundary to $\mu_r + Q = 0$ leading to $r = \text{Int}[\sqrt{2(\mu_0 + |J_i - J_f|)/K}] \simeq 22$. The corresponding $T_0 = 2r/J_f \simeq 220U^{-1}$ is quite close to the numerical value obtained in Fig. 2.
- [22] T. W. B. Kibble, J. Phys. A **9**, 1387 (1976); W. H. Zurek, Nature (London) **317**, 505 (1985); A. Polkovnikov, Phys. Rev. B **72**, 161201(R) (2005).
- [23] S. Mondal, D. Pekker, and K. Sengupta, Europhys. Lett., **100**, 60007 (2012).
- [24] Y. S. Patil, L. M. Aycock, S. Chakram, M. Vengalattore, [arXiv:1404.5583](#) (unpublished).